ORGANOMETALLICS

pubs.acs.org/Organometallics Article

Phospholane-Based Ligands for Chromium-Catalyzed Ethylene Tri- and Tetramerization

Scott D. Boelter, Dan R. Davies, Peter Margl, Kara A. Milbrandt, Darrek Mort, Britt A. Vanchura, II, David R. Wilson, Molly Wiltzius, Mari S. Rosen,* and Jerzy Klosin*

Cite This: https://dx.doi.org/10.1021/acs.organomet.9b00722 Read Online

ACCESS | Metrics & More | Article Recommendations | Supporting Information

ABSTRACT: Chromium complexes with bis(phospholane) ligands were synthesized and evaluated for ethylene tetramerization in a high-throughput reactor. Three ligand parameters—the phospholane substituent, the ligand backbone, and the type of phosphine (cyclic vs acyclic)—were investigated. The size of the phospholane substituent was found to impact the selectivity of the resulting catalysts, with smaller substituents leading to the production of larger proportions of 1-octene. Changing the ligand backbone from 1,2-phenylene to ethylene did not impact catalysis, but the use of acyclic phosphines in place of the cyclic phospholanes had a detrimental effect on catalytic activity. Selected phospholane-chromium complexes were evaluated in a 300 mL Parr reactor at 70 °C and 700 psi of ethylene pressure, and the ethylene oligomerization performance was consistent with that observed in the smaller, high-throughput reactor. MeDuPhos-$CrCl_3$(THF) (MeDuPhos = 1,2-bis(2,5-dimethylphospholano)-benzene; THF = tetrahydrofuran) gave activity and selectivity for 1-octene (54.8 wt %) similar to the state-of-the-art *i*-PrPNP-$CrCl_3$(THF) (64.0 wt %) (PNP = bis(diphenylphosphino)amine), while EtDuPhos-$CrCl_3$(THF) (EtDuPhos = 1,2-bis(2,5-diethylphospholano)benzene) exhibited even higher activity, with catalyst selectivity shifted toward 1-hexene production (90 wt %). These results are surprising, given the prevalence of the aryl phosphine motif in ligands used in ethylene oligomerization catalysts and the inferior performance of previously reported catalysts with alkyl phosphine-containing ligands.

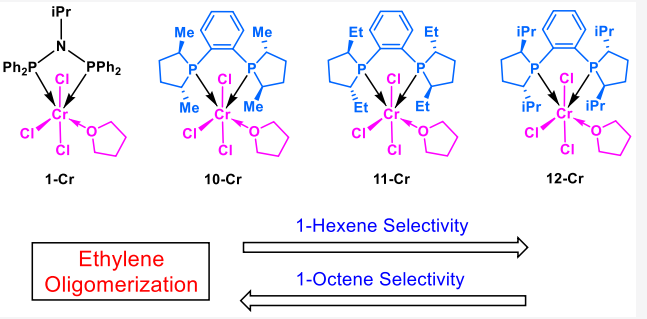

INTRODUCTION

Linear α-olefins are important industrial products made on a very large scale that are used to produce alcohols used to make surfactants and monomers for production of polyalphaolefins, and, most importantly, they are used as comonomers in the production of ethylene/α-olefin copolymers. The world produces over 7000 kilotons per annum (KTA) of linear α-olefins with an annual growth rate of ~5%.[1] Most of the linear α-olefins are produced today via ethylene oligomerization processes that give a wide range of α-olefin products (Schulz–Flory distribution), but interest in on-purpose technologies to produce a single α-olefin has been growing in recent decades.[2,3] Today, both 1-butene and 1-hexene are produced commercially also via selective ethylene di- and trimerization.[1] The most recent addition to on-purpose technologies for α-olefin synthesis is chromium-catalyzed ethylene tetramerization for the selective production of 1-octene. First described by researchers at Sasol Technology in 2004, this process employs a bis(diphenylphosphino)amine (PNP) ligand (**1**, Figure 1) in conjunction with a chromium source and an activator to catalyze the tetramerization of ethylene to 1-octene concurrently with the production of 1-hexene, along with byproducts including cyclic products (methylcyclopentane and methylenecyclopentane), C10–C18 α-olefins, and high-density polyethylene (HDPE) (Scheme 1).[4] Although the production of all byproducts is undesirable, the high-density polyethylene byproduct is particularly unwanted, as it is insoluble in the reaction mixture in this low-temperature process (<100 °C) and can therefore cause significant reactor fouling. Consequently, new ethylene tetramerization catalysts that minimize the formation of all byproducts, and especially HDPE, are highly desirable.

Despite ethylene tetramerization catalysis being known for over a decade, ligand attributes that lead to active catalysts are still not well understood.[2,3,5] The most compelling structure–function relationship that has been described for this catalysis is one relating increased ligand steric bulk to lower 1-octene selectivity.[6] In the absence of additional structure–function relationships to enable rational ligand design, we performed an extensive high-throughput campaign in which over 50

Special Issue: Organometallic Chemistry at Various Length Scales

Received: October 24, 2019

Scheme 1. Major Reaction Products of Chromium-Catalyzed Ethylene Tetramerization

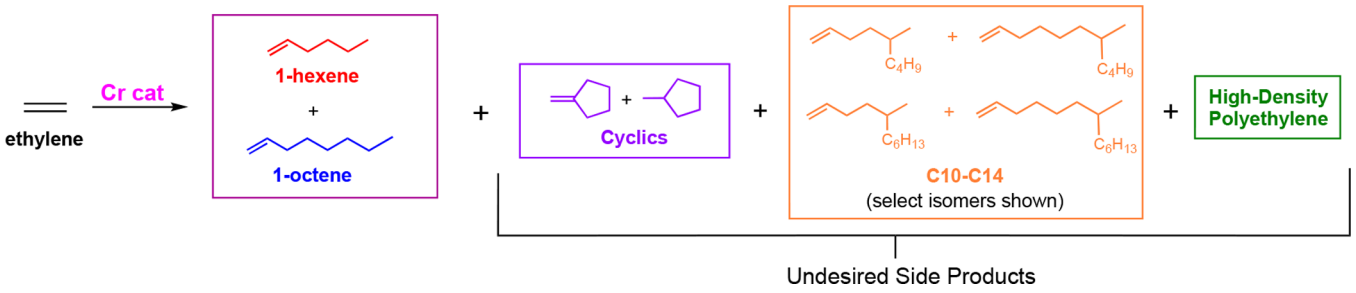

bis(phosphine) ligands were evaluated for ethylene tetramerization with a chromium source with the goal of discovering new ligands that might lead to catalysts with superior selectivity for α-olefins and lower levels of HDPE.[7]

While successful ligands for ethylene tetramerization catalysis typically incorporate diphenylphosphine motifs (Figure 1),[2,4,8−14] this high-throughput study surprisingly led

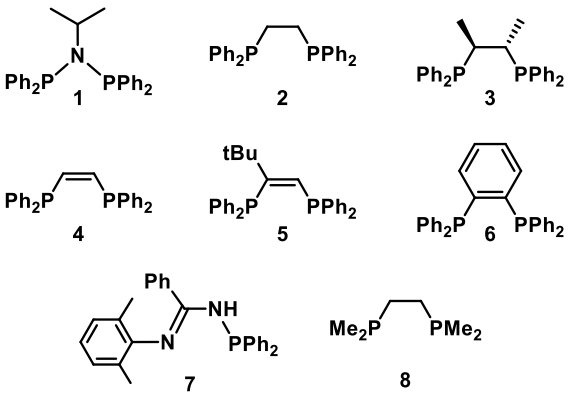

Figure 1. Examples of ligands previously studied for ethylene tri- and tetramerization.

to the identification of bidentate alkyl phosphines as a new class of ligands that lead to active and selective ethylene oligomerization catalysts.[7,15] The 1,2-bis(2,5-dimethylphospholano)benzene (MeDuPhos) ligand (**10**, Figure 2), in which the phosphorus atoms are part of five-

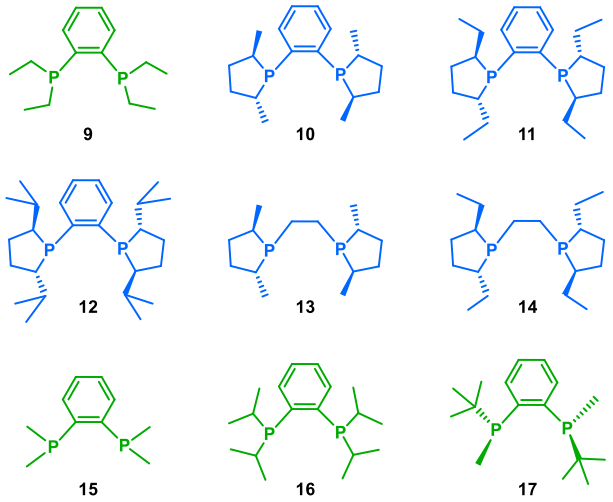

Figure 2. New ligands for ethylene tri- and tetramerization.

membered rings known as phospholanes,[16] was particularly interesting: the MeDuPhos-based catalyst exhibited a combined 1-hexene/1-octene selectivity of 81.8 wt %, approaching that of the state-of-the-art *i*-Pr-PNP ligand (**1**) which demonstrated a combined 1-hexene/1-octene selectivity of 86.8 wt % under the conditions used in that study (60 °C, 0.05 μmol catalyst loading, 500 psi ethylene).[7] Furthermore, with an HDPE selectivity of 3.5 wt % under these conditions, the MeDuPhos ligand (**10**) led to a catalyst with one of the lowest levels of polyethylene formation outside of the PNP ligand family.[7]

The discovery of the MeDuPhos ligand (**10**) as being capable of supporting ethylene tetramerization in conjunction with $CrCl_3(THF)_3$ (THF = tetrahydrofuran) under in situ catalyst formation conditions in the high-throughput study prompted us to perform an investigation into ethylene oligomerization of Cr-based catalysts containing electron-rich phosphine ligands (**9**−**17**). In this paper, three key ligand parameters—the phospholane substituent, the ligand backbone, and the type (cyclic vs acyclic) of electron-rich phosphine—are investigated, and additional mechanistic insights into ethylene tetramerization catalysis are described.

RESULTS AND DISCUSSION

While the high-throughput discovery work was performed with an in situ-formed precatalyst system (in which the ligand was mixed with $CrCl_3(THF)_3$ in methylcyclohexane),[7] a well-defined precatalyst was desired for further investigations. Consequently, a preformed chromium complex was synthesized by reacting the MeDuPhos ligand (**10**) with $CrCl_3(THF)_3$ in tetrahydrofuran at 60 °C for 16 h (Scheme 2). The resulting blue solid was characterized via heteronuclear

Scheme 2. Synthesis of MeDuPhos-$CrCl_3$(THF) (10-Cr)

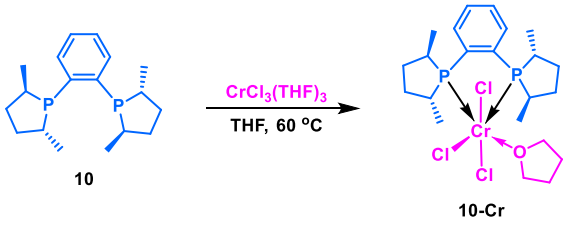

NMR spectroscopy, crystallographic techniques, and combustion elemental analysis. While the MeDuPhos ligand (**10**) exhibits a sharp resonance in the ^{31}P NMR spectrum at δ 2.68, upon complexation no resonances are visible (even when the spectral window is expanded) due to the proximity of the paramagnetic Cr(III) center to the phosphorus atoms (Supporting Information Figure S6a).[17] The paramagnetic

https://dx.doi.org/10.1021/acs.organomet.9b00722
Organometallics XXXX, XXX, XXX−XXX

Cr(III) center also affected the ^{1}H NMR spectrum of the complex, in which only broad resonances in the baseline were observed (Supporting Information Figure S8). The limited information obtained from NMR spectroscopic analyses made the use of other characterization techniques critical for identification of the reaction product. X-ray crystallography performed on a single crystal of this material revealed the structure to be MeDuPhos-$CrCl_3$(THF) (**10-Cr**, Figure 3).[18]

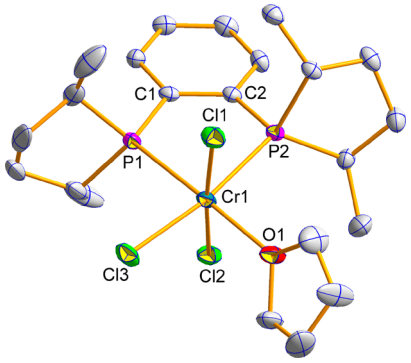

Figure 3. Molecular structure of (*R*,*R*)-MeDuPhos-$CrCl_3$(THF) (**10-Cr**). Thermal ellipsoids are shown at 50% probability, and hydrogen atoms are omitted for clarity. Selected bond distances (Å) and angles (deg): Cr−P1 = 2.4266(9), Cr−P2 = 2.4666(8), Cr−Cl1 = 2.2966(8), Cr−Cl2 = 2.3107(9), Cr−Cl3 = 2.3253(9), Cr−O1 = 2.085(2), P1−Cr1−P2 = 81.85(3), Cr1−P1−C1 = 109.52(9), P1−C1−C2 = 119.5(2), C1−C2−P2 = 118.8(2), C2−P2−Cr1 = 107.72(9). CCDC 1958682.

Powder X-ray diffraction analysis on the bulk material confirmed that the single crystal selected for X-ray diffraction analysis was representative (see Supporting Information Figures S35−S38). Additional confirmation of the bulk composition came from combustion elemental analysis, for which the experimentally obtained values were within 0.4% of those calculated for MeDuPhos-$CrCl_3$(THF) (**10-Cr**). Chromium complexes from ligands **9** and **11**−**17** were also prepared and characterized by combustion elemental analysis, NMR spectroscopy, and single-crystal X-ray crystallography. Molecular structures for EtDuPhos-$CrCl_3$(THF) (**11-Cr**), *i*-PrDuPhos-$CrCl_3$(THF) (**12-Cr**), and $C_6H_4(PEt_2)_2$-$CrCl_3$(THF) (**9-Cr**) are presented in Figures 4, 5, and 6, respectively, whereas molecular structures of **13-Cr**, **14-Cr**, and **17-Cr** are shown in Supporting Information Figures S16, S19, and S26, respectively.

All complexes show a distorted octahedral orientation around the Cr atom with the P1−Cr−P2 bite angle for DuPhos complexes **10-Cr**−**12-Cr** in the range of 80.7−82.4°, which is a significantly wider angle than that in the analogous *i*-Pr-PNP complex **1-Cr** (65.5°, see Supporting Information Figure S3 for the molecular structure of **1-Cr**). The Cr−P bond distances are in the 2.427−2.503 Å range for **10-Cr**−**12-Cr**, which is very similar to those found in **1-Cr** (2.424−2.553 Å). The five atoms of the metallacycle, Cr1−P1−C1−C2−P2, are nearly coplanar with the maximum deviations from the least-squares plane being 0.13 Å (for P1), 0.14 Å (for P1), and 0.14 Å (for P2) for **10-Cr**, **11-Cr**, and **12-Cr**,[19] respectively. The planarity of the five atoms of the Cr1−P1−C1−C2−P2 metallacycle can also be observed in complex **4-Cr**,[20] where the phospholanes are replaced by diphenylphosphine units. In contrast, the metallacycle in the corresponding **9-Cr** complex

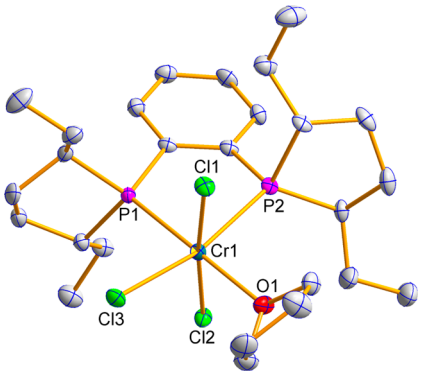

Figure 4. Molecular structure of (*R*,*R*)-EtDuPhos-$CrCl_3$(THF) (**11-Cr**). Thermal ellipsoids are shown at 50% probability, and hydrogen atoms are omitted for clarity. Selected bond distances (Å) and angles (deg): Cr−P1 = 2.4380(9), Cr−P2 = 2.4747(9), Cr−Cl1 = 2.3163(8), Cr−Cl2 = 2.2971(9), Cr−Cl3 = 2.3081(8), Cr−O1 = 2.100(2), P1−Cr1−P2 = 81.63(3), Cr1−P1−C1 = 108.86(10), P1−C1−C2 = 119.8(2), C1−C2−P2 = 119.1(2), C2−P2−Cr1 = 107.65(9). CCDC 1958677.

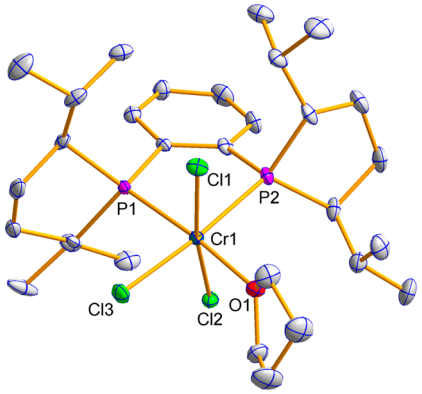

Figure 5. Molecular structure of (*S*,*S*)-*i*-PrDuPhos-$CrCl_3$(THF) (**12-Cr**). Thermal ellipsoids are shown at 50% probability, and hydrogen atoms are omitted for clarity. Selected bond distances (Å) and angles (deg): Cr−P1 = 2.4625(15), Cr−P2 = 2.5027(15), Cr−Cl1 = 2.3163(8), Cr−Cl2 = 2.2971(9), Cr−Cl3 = 2.3192(15), Cr−O1 = 2.135(4), P1−Cr1−P2 = 81.59(5), Cr1−P1−C1 = 109.36(18), P1−C1−C2 = 119.0(4), C1−C2−P2 = 120.2(4), C2−P2−Cr1 = 106.35(17). CCDC 1960323.

shows slightly higher deviation from planarity with the maximum deviation from the least-squares plane being 0.2 Å (for P1). In **9-Cr**, the Cr atom is puckered up above the plane formed by the C_6H_4 bridge, P1, and P2 atoms as is evidenced by the dihedral angle of 22.3° (**9-Cr**) between the planes defined by P1−Cr−P2 and P1−C1−C2−P2.

The largest structural difference between phospholane-based complexes **10-Cr**−**12-Cr** and nonphospholane complexes **4-Cr** and **9-Cr** is seen in the C−P−C bond angles that are not part of a metallacycle in the latter two complexes. The C(Et)−P−C(Et) and C(Ph)−P−C(Ph) bond angles in **9-Cr** (101.9°/101.6°) and **4-Cr** (104.8°/105.9°), respectively, are noticeably larger than the corresponding bond angles in **10-Cr**−**12-Cr**, which vary in the range between 92.9° and 95.6°. However, these bond angle differences at phosphorus atoms do not seem to affect ligand coordination and its configuration at the Cr center. Structurally and electronically, the MeDuPhos ligand (**10**) is quite different from ligands previously employed for ethylene oligomerization with chromium.

https://dx.doi.org/10.1021/acs.organomet.9b00722
Organometallics XXXX, XXX, XXX−XXX

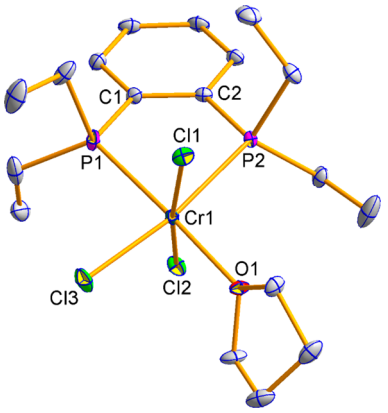

Figure 6. Molecular structure of $C_6H_4(PEt_2)_2$-$CrCl_3(THF)$ (**9-Cr**). Thermal ellipsoids are shown at 50% probability, and hydrogen atoms are omitted for clarity. Selected bond distances (Å) and angles (deg): Cr−P1 = 2.4321(5), Cr−P2 = 2.4836(5), Cr−Cl1 = 2.3323(5), Cr−Cl2 = 2.3069(5), Cr−Cl3 = 2.3176(5), Cr−O1 = 2.0833(12), P1−Cr1−P2 = 80.793(16), Cr1−P1−C1 = 108.10(5), P1−C1−C2 = 119.12(12), C1−C2−P2 = 119.32(12), C2−P2−Cr1 = 106.63(5). CCDC 1958681.

While most ligands used in this catalysis are based on a diphenylphosphine motif (Figure 1), the MeDuPhos ligand (**10**) comprises two dimethylphospholane groups. This should make the MeDuPhos ligand (**10**) considerably more electron-rich than the *i*-Pr-PNP ligand (**1**), and two sets of experiments were performed to probe this difference. First, competition reactions, as illustrated in Scheme 3, were performed. The *i*-Pr-PNP-$CrCl_3(THF)$ complex (**1-Cr**) was synthesized in a similar manner to the MeDuPhos-$CrCl_3(THF)$ complex (**10-Cr**) described above. A chloroform-*d* solution of MeDuPhos ligand (**10**) was then added to a chloroform-*d* solution containing the *i*-Pr-PNP-$CrCl_3(THF)$ complex (**1-Cr**), resulting in almost complete disappearance of the ^{31}P NMR resonance corresponding to the MeDuPhos ligand (**10**) and the appearance of the *i*-Pr-PNP ligand's (**1**) resonance within 10 min (98% conversion), indicative of the rapid coordination of MeDuPhos (**10**) and the concomitant release of *i*-Pr-PNP (**1**; Scheme 3, Supporting Information Figure S34). Conversely, when a solution of *i*-Pr-PNP ligand (**1**) was added to a solution of the preformed MeDuPhos-$CrCl_3(THF)$ (**10-Cr**) complex, no evidence of *i*-Pr-PNP coordination and MeDuPhos release was observed even after 24 h (Scheme 3, Supporting Information Figure S34).

As another means of assessing the electronics of the MeDuPhos (**10**) and *i*-Pr-PNP (**1**) ligands, chromium carbonyl complexes with these ligands were prepared, and IR carbonyl stretching frequencies were evaluated. The *i*-Pr-PNP-$Cr(CO)_4$ (**1-Cr-(CO)$_4$**),[21] $C_6H_4(PPh_2)_2$-$Cr(CO)_4$ (**6-Cr-(CO)$_4$**), and MeDuPhos-$Cr(CO)_4$ (**10-Cr(CO)$_4$**; Scheme 4)

Scheme 4. Synthesis of (*S*,*S*)-MeDuPhos-$Cr(CO)_4$ (10-$Cr(CO)_4$)

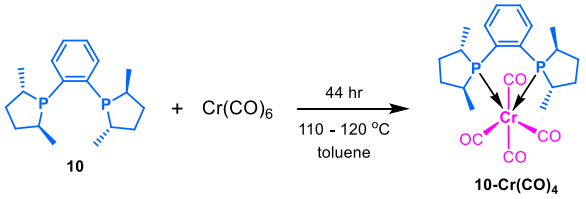

complexes were synthesized in 72%, 84%, and 68% yields, respectively, by heating ligands **1**, **6**, and **10** with an excess of $Cr(CO)_6$ in toluene at 110−120 °C for 2−5 days (see Supporting Information for characterization details including molecular structures of **1-Cr(CO)$_4$**, **6-Cr(CO)$_4$**, and **10-Cr(CO)$_4$**, Supporting Information Figures S28, S33, and S30). Because of the different backbone between **1-Cr(CO)$_4$** (amine bridge) and **10-Cr(CO)$_4$** (1,2-phenylene bridge) and to serve as an additional point of reference, **6-Cr(CO)$_4$**, which contains a 1,2-phenylene bridge, was also synthesized. IR spectra for the three complexes were acquired and overlaid to compare the position of the highest[21] CO stretching frequencies (Figure 7). **10-Cr(CO)$_4$** exhibits the lowest CO stretching frequency at 1995 cm^{-1}, consistent with MeDuPhos (**10**) being the most electron-donating ligand of the three. Interestingly, the *i*-Pr-PNP ligand (**1**) appears to be a more donating ligand than ligand **6**, as evidenced by the CO stretching frequencies at 1999 and 2007 cm^{-1}, respectively (Figure 7). Full IR spectra are shown in Supporting Information Figures S39−S42. These experiments provide further support that the MeDuPhos ligand (**10**) is indeed more electron-rich than the *i*-Pr-PNP ligand (**1**). Because the MeDuPhos ligand (**10**) is capable of leading to a high-activity ethylene tetramerization catalyst with

Scheme 3. Competition Reactions Between *i*-Pr-PNP (1) and MeDuPhos (10) Ligands

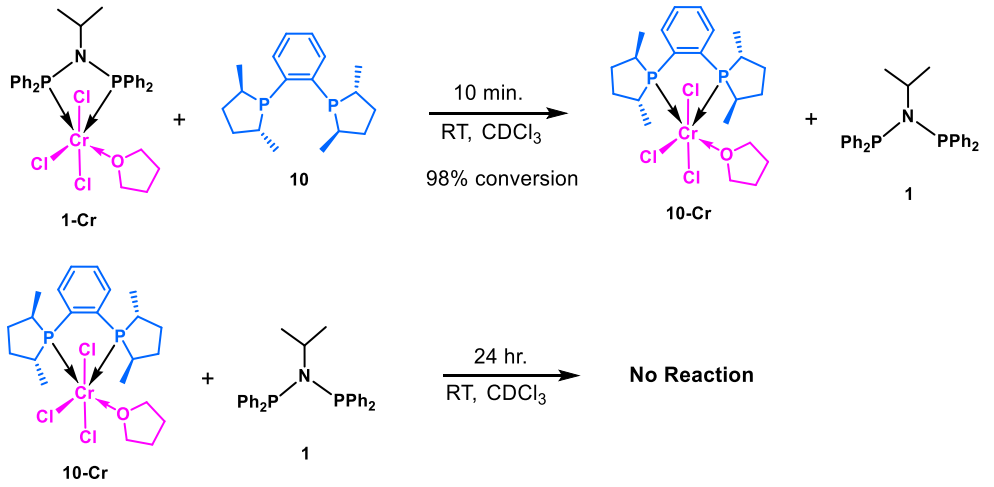

https://dx.doi.org/10.1021/acs.organomet.9b00722
Organometallics XXXX, XXX, XXX−XXX

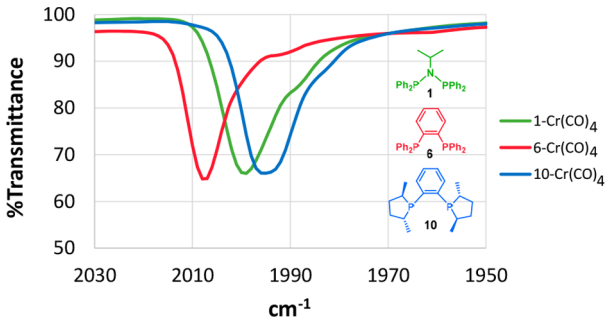

Figure 7. Overlay of IR spectra (CO stretching frequency region) for **1-Cr(CO)$_4$**, **6-Cr(CO)$_4$**, and **10-Cr(CO)$_4$**.

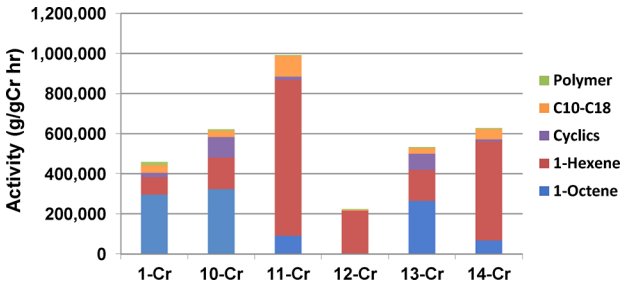

Figure 8. Performance of MeDuPhos-CrCl$_3$(THF) (**10-Cr**), EtDuPhos-CrCl$_3$(THF) (**11-Cr**), *i*-PrDuPhos-CrCl$_3$(THF) (**12-Cr**), MeBPE-CrCl$_3$(THF) (**13-Cr**), and EtBPE-CrCl$_3$(THF) (**14-Cr**) precatalysts for ethylene oligomerization compared to the benchmark *i*-Pr-PNP-CrCl$_3$(THF) (**1-Cr**) catalyst system.

good selectivity, electron-rich ligands should not be discounted in future catalyst development efforts.

With the preformed MeDuPhos-CrCl$_3$(THF) (**10-Cr**) in hand, we evaluated it for ethylene tetramerization in the high-throughput reactor. High-throughput experiments were performed in tared glass inserts in a 24-well stainless-steel reactor housed entirely in a nitrogen-purged glovebox. Ethylene oligomerization reactions were performed at 45 °C and 500 psi ethylene in methylcyclohexane for 30 min. A large excess (1000 equiv) of modified methylaluminoxane (MMAO-3A) was used as the activator.[22] Nonane was included as an internal standard in each reaction vessel to enable quantification of liquid reaction products by gas chromatography. At the end of the reaction the glass inserts were removed from the wells of the reactor, a small aliquot was removed for GC analysis, the liquid products and solvent in the inserts were devolatilized, and the inserts were reweighed to obtain the mass of polymer produced. We found that the preformed MeDuPhos-CrCl$_3$(THF) (**10-Cr**) precatalyst led to a catalyst with selectivity for α-olefin products comparable to that derived from the in situ generated MeDuPhos/CrCl$_3$(THF)$_3$ precatalyst (**10**/CrCl$_3$(THF)$_3$),[7] but with considerably higher activity and improved HDPE selectivity (1.3 vs 8.4 wt %). Notably, the catalyst derived from preformed MeDuPhos-CrCl$_3$(THF) (**10-Cr**) had similar activity and superior HDPE selectivity (1.3 vs 2.0 wt %) to that of the benchmark *i*-Pr-PNP/CrCl$_3$(THF)$_3$ catalyst, (Table 1, Figure 8). These results were confirmed on a larger scale in a 300 mL semibatch Parr reactor (vide infra). Having established the excellent performance of the MeDuPhos-CrCl$_3$(THF) (**10-Cr**) precatalyst, we sought a greater understanding of how ligand structure influences catalytic activity. Three ligand structural parameters were selected for modification: the phospholane substituent, the ligand backbone, and the cyclic phospholane structure (comparison of cyclic vs acyclic phosphines). To examine the influence of the phospholane substituent on catalysis, two additional complexes with commercially available EtDuPhos (**11**) and *i*-PrDuPhos (**12**) ligands were synthesized in an analogous fashion to the MeDuPhos-CrCl$_3$(THF) (**10-Cr**) precatalyst. Single-crystal X-ray diffraction studies revealed that the chromium complexes with EtDuPhos and *i*-PrDuPhos ligands are also monomeric ligand-CrCl$_3$(THF) complexes (Figures 4 and 5), and combustion elemental analysis confirmed bulk composition. These EtDuPhos-CrCl$_3$(THF) (**11-Cr**) and *i*-PrDuPhos-CrCl$_3$(THF) (**12-Cr**) precatalysts were evaluated under the same conditions as **1-Cr** and **10-Cr** precatalysts (Table 1, Figure 8). While the activities of the preformed *i*-Pr-PNP-CrCl$_3$(THF) complex (**1-Cr**) and the *i*-Pr-PNP (**1**)/CrCl$_3$(THF)$_3$ in situ-formed catalyst were comparable, among the catalysts with DuPhos family ligands, the preformed complexes always led to more active catalysts than the analogous in situ-formed catalysts. This is particularly dramatic for the catalysts employing *i*-PrDuPhos (**12**/CrCl$_3$(THF)$_3$ and **12-Cr**), where the in situ-formed catalyst was completely inactive. We hypothesize that because the DuPhos ligands are more electron-rich than the PNP ligand (vide supra), they are more likely to interact with the excess alkyl aluminum in the MMAO-3A, rather than binding to the chromium, which results in lower catalytic activity. In addition to higher activities, catalysts with DuPhos ligands using preformed complexes as precatalysts consistently led to lower HDPE formation.

A relationship emerged between the size of the phospholane substituent and the octene selectivity: the precatalyst **10-Cr** with the MeDuPhos ligand—the ligand with the smallest phospholane substituents—gave 52.0 wt % 1-octene and 25.3 wt % 1-hexene, while **11-Cr**—the precatalyst with the EtDuPhos ligand containing larger phospholane substituents—gave only 9.2 wt % 1-octene and 78.2 wt % 1-hexene (Table 1 and Figure 8). When the steric bulk of ligand

Table 1. Ethylene Oligomerization Performance of 1-Cr and 9-Cr−17-Cr in a High-Throughput Reactor[a]

	1-Cr	10-Cr	11-Cr	12-Cr	13-Cr	14-Cr	16-Cr	9-Cr	15-Cr	17-Cr
product yield (g)	1.2	1.6	2.6	0.6	1.4	1.6	0.05	0.5	0.05	0.4
total activity (kg product/g Cr hr)	459	623	992	224	534	628	18	178	18	168
1-octene (wt %)	64.0	52.0	9.2	0.5	49.6	10.8	16.6	40.1	21.1	0.10
1-hexene (wt %)	19.5	25.3	78.2	95.7	28.8	78.7	5.5	29.0	34.5	96.0
cyclics (wt %)	4.7	16.4	1.7	0.09	15.26	1.6	15.7	16.0	5.6	0.07
HDPE (wt %)	3.6	1.3	0.5	2.0	1.1	0.9	43.9	2.6	35.0	2.7

[a]45 °C, 500 psi ethylene, 30 min reaction, 0.1 μmol of Cr, total starting volume = 5 mL, solvent = methylcyclohexane, MMAO-3A/Cr = 1000:1, data are the average of two replicates, cyclics (wt %) is the combined methylenecyclopentane and methylcyclopentane wt %.

https://dx.doi.org/10.1021/acs.organomet.9b00722
Organometallics XXXX, XXX, XXX−XXX

substituents was increased further in **12-Cr** with the use of the *i*-PrDuPhos ligand, the 1-octene selectivity diminished to a mere 0.5 wt %, and 1-hexene was the predominant product (95.7 wt %). The decrease in 1-octene selectivity as the phospholane ligand substituents increase in size is consistent with the previous observations of such relationships between ligand steric bulk and 1-octene/1-hexene selectivity established within the PNP-Cr catalyst family.[6] It is of value to know, however, that this phenomenon is relevant across multiple ligand families and not only for the PNP ligands that were previously studied.

Having observed experimentally that the steric bulk of the DuPhos ligand influences the selectivity, we were interested to know whether we could also observe this computationally and, perhaps, use a steric descriptor to predict 1-octene selectivity of a new catalyst. The descriptor (θ) published[6] by researchers from Sasol is *not* directly applicable outside the PNP ligand family. Consequently, we attempted to apply the "percent buried volume" ($\%V_{bur}$) steric descriptor, which has previously been successfully used to describe steric properties of phosphine and *N*-heterocyclic carbene ligands for other systems.[23,24] The $\%V_{bur}$ steric descriptor involves placing the metal center of the species of interest at the center of a sphere of defined radius (typically 3.5 Å), and the percent volume of the sphere occupied by the ligand is measured as the $\%V_{bur}$ value. Unfortunately, we were not able to use this method[25] to obtain a strong correlation between observed 1-octene versus 1-hexene selectivity and the steric bulk descriptor, $\%V_{bur}$ (see Supporting Information). Even after increasing the size of the sphere to 5 Å to account for the position of the phospholane substituents farther than 3.5 Å from the metal center, we were not able to identify a correlation between ligand sterics and observed selectivity. This lack of correlation was surprising, since the ligand size increase in the series of DuPhos ligands (Me vs Et vs *i*-Pr) was evident.

To evaluate the effect of the ligand backbone on catalysis, the activity and selectivity of the DuPhos ligands, which have 1,2-phenylene backbones, were compared to those of analogous bis(phospholane)ethane (BPE) ligands. Chromium complexes with the commercially available MeBPE and EtBPE ligands were synthesized in an analogous fashion to the MeDuPhos-$CrCl_3$(THF) complex (**10-Cr**) described above. Comparison of the precatalysts with BPE ligands (**13-Cr** and **14-Cr**) with those with DuPhos ligands (**10-Cr**, **11-Cr**, and **12-Cr**) revealed many similarities between the two ligand classes. Consistent with the hypothesis that steric bulk is a significant factor in determining the 1-octene/1-hexene ratio, the selectivities of the catalysts employing MeDuPhos (**10**) and MeBPE (**13**) ligands were comparable, and those employing EtDuPhos (**11**) and EtBPE (**14**) were also comparable (Figure 8).

Finally, it was not obvious that the cyclic phospholane structure was necessary for the ethylene oligomerization behavior observed for the bis(phospholane) ligands evaluated thus far. In fact, in the previous high-throughput study in which in situ catalyst formation was employed, acyclic phosphines with ethyl substituents were identified as leading to active tetramerization catalysts, albeit with lower activities than that from the *i*-Pr-PNP system (**1-Cr**).[7] Having learned that preformed precatalysts are superior to in situ catalyst formation for catalysts employing DuPhos ligands, a series of chromium complexes comprising ligands with acyclic phosphines (**9**, **15**, **16**, **17**) were synthesized and evaluated for ethylene oligomerization catalysis (Figure 9). Interestingly, of the preformed complexes evaluated, only that with the

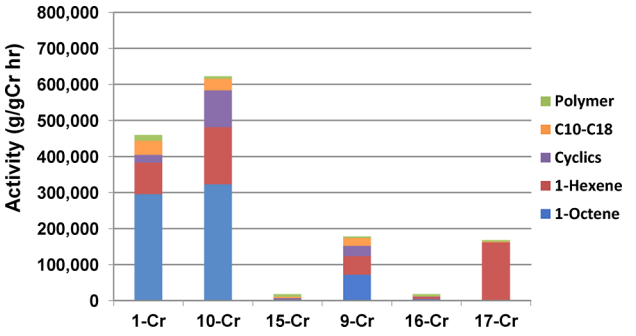

Figure 9. Performance of **9-Cr**, **15-Cr**, **16-Cr**, and **17-Cr** precatalysts for ethylene oligomerization compared to the *i*-Pr PNP-$CrCl_3$(THF) (**1 Cr**) and MeDuPhos $CrCl_3$(THF) (**10-Cr**) catalyst systems.

diethylphosphine ligand (**9**) led to an active tetramerization catalyst, albeit with moderate activity. The selectivity of this catalyst was not optimal, yielding only 40.1 wt % 1-octene. The catalyst with the methyl(*t*-butyl)phosphine ligand (**17**) gave a hexene-selective catalyst, as expected due to the high level of steric bulk of the phosphine substituents, with moderate activity (168 kg products/g Cr hr). It was surprising to us that the acyclic phosphine ligands evaluated did not give catalysts with activities comparable to those with cyclic phospholane ligands, and the reason behind this difference in catalytic behavior is not yet fully understood. It is clear, however, that bis(phospholanes) are a privileged ligand class for ethylene oligomerization.

Having established the efficacy of DuPhos-based catalysts for ethylene oligomerization on the small scale of a high-throughput reactor, a confirmation of this activity was sought on a larger scale. To this end, the preformed *i*-Pr-PNP-$CrCl_3$(THF) (**1-Cr**), MeDuPhos-$CrCl_3$(THF) (**10-Cr**), and EtDuPhos-$CrCl_3$(THF) (**11-Cr**) complexes were evaluated in a 300 mL semibatch Parr reactor. The semibatch reactor was equipped with a thermocouple to monitor the temperature of the reaction mixture and an internal cooling coil that allows for effective temperature control. The reactor was brought to the desired reaction temperature and pressure, 70 °C and 700 psi ethylene, prior to the introduction of the catalyst solution. This was enabled through the use of a shot tank, a small vessel connected to the reactor body that was pressurized with nitrogen to transfer the catalyst solution into the reactor body. Ethylene was fed to the reactor on demand to maintain the 700 psi reactor pressure during the course of the 30 min reaction. After the reaction, the reactor was disconnected from all lines and brought into a nitrogen-purged glovebox, where the reactor was opened, the liquid products were sampled for gas chromatographic analysis, and the polymer byproduct was removed and dried for weighing.

While the high-throughput experiments (Table 1) used equivalent loadings for all catalysts, catalyst loadings for semibatch experiments were adjusted to allow production of products within a 10−30 g scale while keeping the reaction exotherm within 3 °C. For example, when we evaluated **11-Cr** at 1 μmol loading, the reaction exotherm exceeded 20 °C.

The trends in catalyst activity and selectivity in the high-throughput reactor were also observed in the results from the semibatch reactor. At this larger scale, the activities of *i*-Pr-

https://dx.doi.org/10.1021/acs.organomet.9b00722
Organometallics XXXX, XXX, XXX−XXX

PNP-$CrCl_3$(THF) (**1-Cr**) and MeDuPhos-$CrCl_3$(THF) (**10-Cr**) were comparable, with both ∼1 000 000 g product/g Cr hr. However, EtDuPhos-$CrCl_3$(THF) (**11-Cr**) gave a catalyst with an activity approximately double that, ∼2 000 000 g product/g Cr hr (Table 2). With respect to catalyst selectivity,

Table 2. Activities and Selectivities of 1-Cr, 10-Cr, and 11-Cr in a 300 mL Semi-Batch Reactor[a]

	1-Cr	10-Cr	11-Cr
catalyst loading (μmol)	1	0.5	0.2
product yield (g)	27.8	11.9	11.2
total activity (g product/g Cr hr)	1 070 000	915 000	2 150 000
1-octene (wt %)	66.4	54.8	16.0
1-hexene (wt %)	22.2	29.9	77.1
cyclics (wt %)	4.1	11.2	3.0
HDPE (wt %)	2.0	1.0	0.6

[a]70 °C, 700 psi ethylene, 30 min reaction, solvent = methylcyclohexane, MMAO-3A/Cr = 1000:1, cyclics (wt %) is the combined methylenecyclopentane and methylcyclopentane wt %.

the DuPhos-based catalysts **10-Cr** and **11-Cr** gave lower selectivities for the undesired HDPE byproduct of 1.0 and 0.6 wt %, respectively, compared to 2.0 wt % for **1-Cr**. As we observed in the high-throughput reactor, MeDuPhos-$CrCl_3$(THF) (**10-Cr**) gave primarily an ethylene tetramerization catalyst with a 1-octene selectivity of 54.8 wt %, while EtDuPhos-$CrCl_3$(THF) (**11-Cr**) gave primarily an ethylene trimerization catalyst with a 1-hexene selectivity of 77 wt %. With respect to the combined selectivity of 1-octene and 1-hexene, the useful products of this reaction, MeDuPhos-$CrCl_3$(THF) (**10-Cr**) and EtDuPhos-$CrCl_3$(THF) (**11-Cr**) performed admirably, with selectivities of 84.7 and 93.1 wt %, respectively, compared to 88.6 wt % for the state-of-the-art *i*-Pr-PNP-$CrCl_3$(THF) (**1-Cr**).

An analysis of the ethylene oligomerization reaction products derived from the catalysts presented here provides additional insights into the ethylene tetramerization mechanism. As illustrated in Figure 10, there is a clear correlation

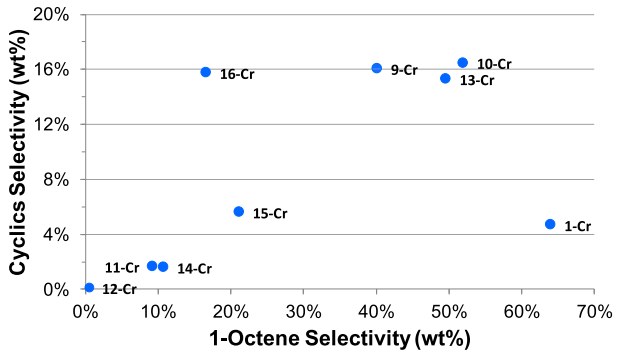

Figure 10. Cyclics vs 1-octene selectivities for all catalysts studied. Data from Table 1.

between the combined selectivity of the cyclic byproducts and the selectivity for 1-octene, with catalysts more selective for 1-octene also tending to produce higher levels of cyclics. While the catalyst with the *i*-Pr-PNP ligand (**1**), which shows high 1-octene selectivity, but does not give a high level of cyclic products, does not fall along the same trend line as the other catalysts evaluated here, this catalyst still produces more cyclics than highly selective 1-hexene catalysts. For example, catalysts **10-Cr**, **11-Cr**, and **12-Cr** exhibit 1-octene selectivities of 52, 9.2, and 0.5 wt % while producing 16.4, 1.7, and 0.09 wt % of cyclics, respectively. The overall trend strongly suggests that the production of 1-octene and the cyclic products is mechanistically linked. Such an observation was made by Cloate and co-workers[6] when evaluating various derivatives of the *i*-Pr-PNP ligand that exhibit a range of 1-octene selectivities. More recently Britovsek and co-workers[26] studied 1-octene selectivity as a function of ethylene pressure using a $CrCl_3(THF)_3$/*i*-Pr-PNP(**1**)/MAO catalyst system. They observed that, at lower ethylene pressures where the 1-octene selectivity is lower, the proportions of cyclic products produced are also lower. Analysis of kinetics data revealed that 1-octene and cyclics formation show the same ethylene dependence, which is different from that of 1-hexene. This information, coupled with density functional theory (DFT) calculations, led Britovsek et al. to propose a modified mechanism for 1-hexene and 1-octene production that also accounts adequately for the main byproducts formed during ethylene oligomerization (Scheme 5).

The oxidative coupling of two ethylene molecules with a Cr^n center yields a chromacyclopentane (**B**), into which a third ethylene inserts, yielding a chromacycloheptane (**C**) (Scheme 5). Sterically bulky ligands impede the insertion of an additional ethylene into the chromacycloheptane intermediate and make it more likely to undergo a concerted 3,7-hydride shift (**D**) giving 1-hexene. Ethylene association with chromacycloheptane **C** gives **E**,[27] which is a common intermediate to both 1-octene and cyclic products. The insertion of ethylene into intermediate **E** can lead to the formation of chromacyclononane **F**, which gives 1-octene via a 3,9-hydride shift, or β-H transfer to ethylene can lead to the formation of Cr-ethyl-hexenyl species **G**. Cyclization then leads to the formation of complex **H**, which can then decompose via a β-H abstraction to cyclic products methylenecyclopentane and methylcyclopentane along with ethylene and ethane. This mechanisim explains why the formation of 1-octene and cyclic products is linked. It also explains the observation that catalysts that are highly selective for 1-hexene production give very low levels of cyclic byproducts.[2,8]

The most commonly proposed alternative mechanism[2,3,28,29] for the formation of 1-hexene and the cyclic products involves the formation of a chromium-hexenyl-hydride species **I** (Scheme 6) that arises from β-H elimination from the chromacycloheptane metallacycle **C**. Complex **I** can then either directly eliminate 1-hexene or can cyclize to form **J**, which leads to the cyclic byproducts. However, in this scenario, cyclics production would be expected to increase with 1-hexene formation and not with 1-octene formation as we and others have observed experimentally. Additionally, if the mechanism shown in Scheme 6 were operative, 1-hexene-selective catalysts would be expected to form larger quantities of cyclic products, which is not supported by the experimental data.

The observation that an approximate 1:1 ratio of the two cyclic byproducts methylenecyclopentane and methylcyclopentane is obtained with the PNP/Cr system has led to a variety of mechanistic proposals involving binuclear mechanisms.[30] Although a 1:1 ratio of cyclic products is not inconsistent with the mechanism shown in Scheme 5, this mechanism does not place any constraints on the ratio of these cyclic products, which should be governed by two independent

https://dx.doi.org/10.1021/acs.organomet.9b00722
Organometallics XXXX, XXX, XXX−XXX

Scheme 5. Proposed Mechanism for Chromium-Catalyzed Ethylene Tetramerization

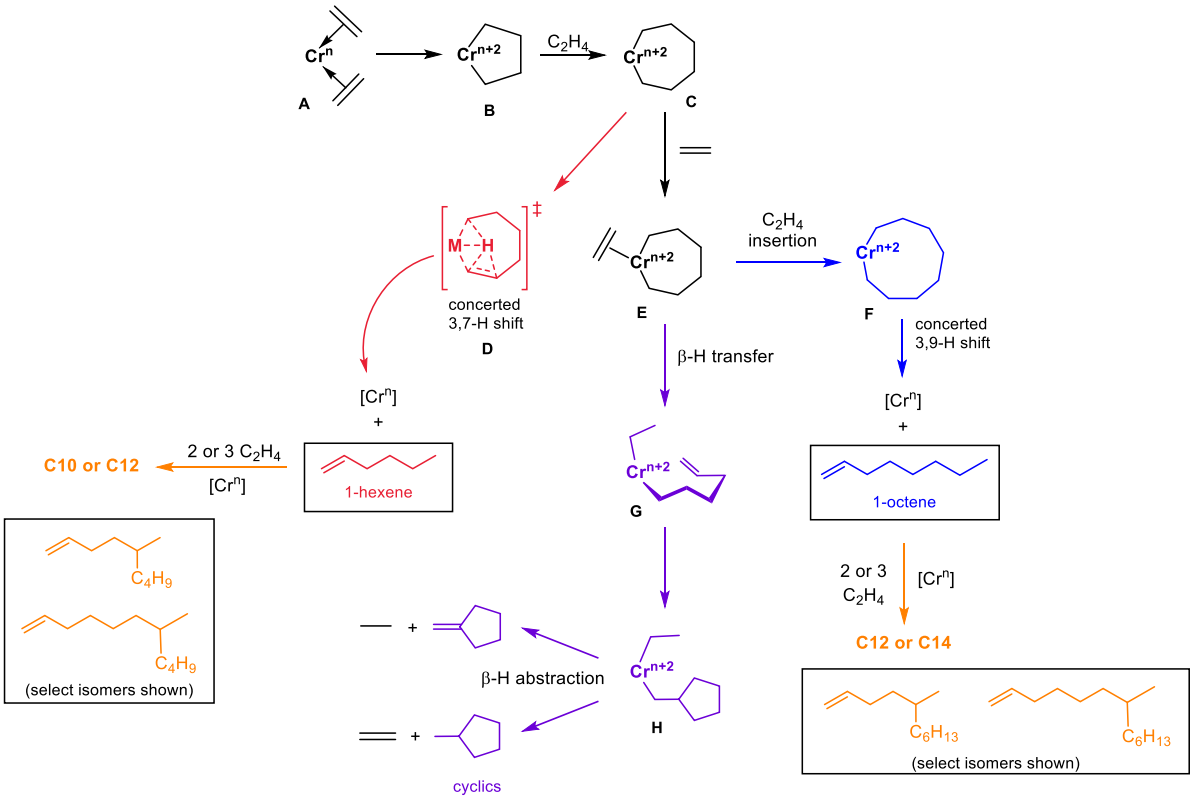

Scheme 6. Alternative Mechanism for the Formation of 1-Hexene and Cyclic Byproducts in Chromium-Catalyzed Ethylene Tetramerization

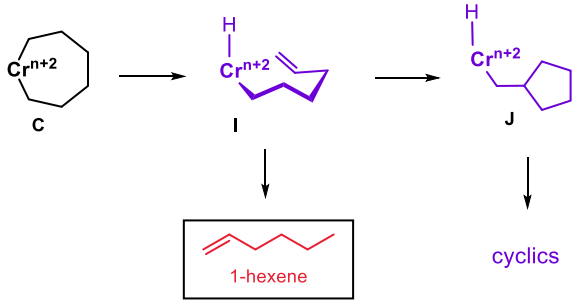

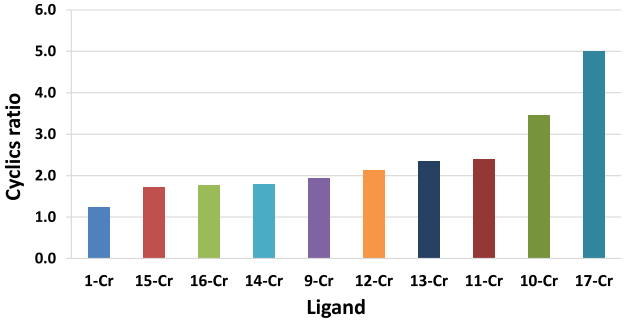

Figure 11. Cyclics ratio (methylenecyclopentane/methylcyclopentane) is ligand-dependent, ranging from ~1 for **1-Cr** (the *i*-Pr-PNP-based catalyst) to 5.0 for **17-Cr**. Conditions given in Table 1.

β-H abstraction transition states. Therefore, for different ethylene oligomerization catalysts, one could expect to observe deviation from 1:1 cyclic product ratios, which has not been previously observed to our knowledge. Interestingly, for the bis(phospholane)- and acyclic dialkylphosphine-based catalysts studied here, we do in fact observe a range of different values for the ratio of methylenecyclopentane to methylcyclopentane (the cyclics ratio, Figure 11). The cyclics ratio varies from 1.25 for the *i*-Pr-PNP-$CrCl_3$(THF) (**1-Cr**) catalyst to 2.3 for **11-Cr** and up to 5.0 for **17-Cr**. These data, displayed in Figure 11, clearly demonstrate that methylenecyclopentane production and methylcyclopentane production are not directly linked to each other and are consistent with the mechanism shown in Scheme 5.

CONCLUSION

In conclusion, we have unexpectedly discovered that the bis(phospholane) motif leads to successful ligands for chromium-catalyzed ethylene tri- and tetramerization despite being more electron-rich than the diphenylphosphine motifs used in many successful ligands for this chemistry. Catalysts comprising DuPhos and BPE ligands exhibited high activities and excellent selectivities in ethylene oligomerization reactions. MeDuPhos-$CrCl_3$(THF) (**10-Cr**) exhibited high activity and selectivity (comparable activity and similar selectivity to the state-of-the-art *i*-Pr-PNP-$CrCl_3$(THF) (**1-Cr**) catalyst), while EtDuPhos-$CrCl_3$(THF) (**11**-Cr) was the most active catalyst in this study, exceeding even the activity of the benchmark *i*-Pr-PNP-$CrCl_3$(THF) (**1-Cr**) catalyst and showing preference for 1-hexene formation. The strong correlation between 1-octene and cyclic byproduct formation as well as the range of cyclic byproducts ratios formed by different catalysts supports a mechanism that involves a common intermediate, ethylene-bound chromacycloheptane, that leads to the formation of both 1-octene and cyclopentane-based (cyclics) byproducts.

https://dx.doi.org/10.1021/acs.organomet.9b00722
Organometallics XXXX, XXX, XXX−XXX

It is evident that bis(phospholanes) are a special ligand class for chromium-catalyzed ethylene oligomerization, and it is likely that additional derivatives based on the phospholane motif might lead to catalysts with even better activity and selectivity. Our results demonstrate that ligands that do not contain the widely used diphenylphosphine motif can be useful for ethylene tri- and tetramerization and that the range of relevant ligand motifs for successful catalysts is much wider than previously thought, which should lead to new research directions and discoveries.

EXPERIMENTAL SECTION

General Methods. All reagents were obtained from commercial sources and used as received unless otherwise noted. All syntheses and manipulations of air-sensitive materials were performed under an inert atmosphere (nitrogen). Solvents (toluene, hexane, diethyl ether) were first saturated with nitrogen and then dried by passage through activated alumina and Q-5 catalyst (available from Engelhard Corporation) prior to use. C_6D_6 was dried over Na/K, and $CDCl_3$ was dried over activated 4 Å molecular sieves before use. NMR spectra were recorded on Varian MR-400, VNMRS-500, and Bruker-400 spectrometers. ^{1}H NMR data are reported as follows: chemical shift (multiplicity (br = broad, s = singlet, d = doublet, t = triplet, q = quartet, p = pentet, and m = multiplet), integration, and assignment). Chemical shifts for ^{1}H NMR data are reported in parts per million downfield from internal tetramethylsilane (TMS, δ scale) using residual protons in the deuterated solvents (C_6D_6, 7.15 ppm: $CDCl_3$, 7.25 ppm) as references. ^{13}C NMR data were determined with ^{1}H decoupling, and the chemical shifts are reported in parts per million versus tetramethylsilane (C_6D_6, 128 ppm, $CDCl_3$, 77 ppm). Elemental analyses were performed at Midwest Microlab, LLC. Syntheses of representative complexes are shown below, and the syntheses of the remaining compounds are given in the Supporting Information. The high-throughput catalyst evaluation procedure can be found in the Supporting Information.[7]

Semi-Batch Reactor Experimental Information. The ethylene tetramerization reactions were conducted in a 300 mL Parr semibatch reactor equipped with a 10 mL catalyst shot tank, an agitator, and a thermocouple. The reactor was heated by an electrical resistive heating mantle, and temperature was controlled through the use of the heating mantle as well as by an internal cooling coil. Both the reactor and the temperature-control system were controlled and monitored by a Camile TG automation system. The nitrogen and ethylene feeds, as well as the methylcyclohexane solvent, were passed through purification columns containing A2 alumina and Q-5 reagents. Chlorobenzene and nonane were passed through activated alumina. The methylcyclohexane, chlorobenzene, and nonane were stored over activated 4 Å molecular sieves.

All reactor manipulations and solution preparations were performed in a nitrogen-purged glovebox. For precatalysts prepared in situ, a solution of 1.2 equiv of the ligand in methylcyclohexane (2 mM) was added in a dropwise fashion to a solution of 1 equiv of the Cr precursor ($CrCl_3(THF)_3$) in chlorobenzene (2 mM), and the resulting solution was stirred for 30 min. For precatalysts comprising preformed ligand-chromium complexes, a solution of the complex was prepared in chlorobenzene (2 mM). Methylcyclohexane (100 mL) was added to the reactor body in a glovebox, along with MMAO-3A (1.77 M in heptane) and nonane (the internal standard for GC analysis). The precatalyst solution was loaded into a 10 mL catalyst shot tank, and the vial and syringes containing the precatalyst solution were washed with 2.5 mL of methylcyclohexane that was added to the shot tank. The reactor was then sealed and removed from the glovebox.

The reactor was then transferred to a reactor stand equipped with the heating mantle, and connections were made to the nitrogen and ethylene feed lines, cooling lines, and a vent line. The reactor was pressure-tested to 750 psi nitrogen. After the pressure test, the reactor was slowly vented to ~10 psi and then slowly heated to 70 °C. When this temperature was reached, ethylene was added through a Brooks thermal mass flow meter to the desired reaction pressure. When the reactor temperature and pressure had stabilized, the catalyst shot tank was pressurized with nitrogen to 200 psi over the reactor pressure, and the precatalyst solution was injected into the reactor, beginning the reaction. Ethylene was fed on demand through the Brooks thermal mass flow controller, and the temperature was controlled by adjusting the mantle temperature and the flow through the internal cooling coil.

After the 30 min reaction time, the ethylene feed was stopped, and the reactor was cooled to 35 °C and then vented at a rate of 1−4 psi per second, until 10 psi was reached. At this point, the reactor was returned to the nitrogen-filled glovebox, where it was unsealed. The contents of the reactor were sampled for gas chromatography (GC) analysis, and then the reactor contents were emptied. The reactor was thoroughly cleaned to remove any polymer not suspended in the solvent. The bulk of the solvent was allowed to evaporate, and the remaining residue was dried in a vacuum oven. The resulting residue was weighed to give the polymer yield for the reaction.

Synthesis of i-Pr-PNP-$CrCl_3$(THF) (1-Cr). A 20 mL vial was charged with solid *N*-(diphenylphosphino)-*N*-(1-methylethyl)-*P*,*P*-diphenyl-phosphinous amide (**1**) (0.100 g, 0.234 mmol) and solid $CrCl_3(THF)_3$ (0.087 g, 0.213 mmol). Toluene (8 mL) was added, and the vial was shaken. A deep blue-black color developed within 5 min, with undissolved solids still present. The reaction mixture was shaken well and was allowed to stand overnight to give a deep blue-black solution with almost no precipitate. The solution was filtered via syringe filter into a 20 mL vial and allowed to stand overnight. Several very large crystals formed. Elemental analysis for iPr-PNP-$CrCl_3$(THF)·toluene: calculated: C, 60.85; H, 5.78; N, 1.87; found: C, 60.28; H, 5.69, N, 1.62%.

Synthesis of Complex 9-Cr. $CrCl_3(THF)_3$ (294.7 mg, 0.79 mmol) was dissolved in 5 mL of THF giving a purple solution. To this solution was added a solution of 200 mg of ligand **9** (0.79 mmol) dissolved in 5 mL of THF. The reaction mixture was allowed to stir overnight at ambient temperature. The reaction mixture was filtered through a disposable frit, and the solvent was removed from the filtrate in vacuo, yielding 66.8 mg of a blue solid. Yield 17.5%. Crystals suitable for a single-crystal X-ray diffraction study were grown by evaporation of a THF/hexanes solution of the compound at ambient temperature. Elemental analysis: Calculated: C, 44.60; H, 6.65. Found: C, 44.12; H, 6.96%.

Synthesis of (R,R)-MeDuPhos-$CrCl_3$(THF) (10-Cr). To a vial containing (*R*,*R*)-MeDuphos (**10**) (0.60 g, 1.96 mmol) and $CrCl_3(THF)_3$ (0.56 g, 1.51 mmol) was added 15 mL of THF. The resulting solution was stirred for 30 min at ambient temperature and then heated for 1 h at 60 °C. The THF was concentrated under formation of crystalline material. The supernatant was pipetted away from the solids. The solids were dried under reduced pressure to give violet-blue crystalline material, 0.4776 g, 59.0%. Crystals suitable for X-ray diffraction analysis were grown by slow evaporation of a THF solution at ambient temperature. Elemental analysis: Calculated: C, 49.22; H, 6.76; Found: C, 49.24; H, 6.69%.

Synthesis of (R,R)-EtDuPhos-$CrCl_3$(THF) (11-Cr). $CrCl_3(THF)_3$ (513 mg, 1.38 mmol) was dissolved in 5 mL of THF giving a purple solution. To this solution was added dropwise a solution of the (*R*,*R*)-EtDuPhos ligand (**11**) (500 mg, 0.60 mmol) dissolved in 5 mL of THF. Almost immediately upon addition of the ligand, the solution color changed to a deep cobalt blue. The reaction mixture was stirred for 8 h (homogeneous solution), and then the solvent was removed in vacuo. The resulting blue solid was dried under vacuum at 60 °C overnight. Yield 506.7 mg, 62%. Crystals suitable for X-ray diffraction analysis were grown by evaporation of a THF/hexanes solution at ambient temperature. Elemental analysis: Calculated: C, 52.67; H, 7.48. Found: C, 52.43; H, 7.26%.

Synthesis of (S,S)-i-PrDuPhos-$CrCl_3$(THF) (12-Cr). $CrCl_3(THF)_3$ (224 mg, 0.60 mmol) was dissolved in 5 mL of THF resulting in a purple solution. To this solution was added dropwise a solution of the (*S*,*S*)-iPrDuPhos ligand (**12**) (250 mg, 0.60 mmol) in 5 mL of THF. Almost immediately upon ligand addition, the solution color changed to a deep cobalt blue. The reaction mixture was stirred

https://dx.doi.org/10.1021/acs.organomet.9b00722
Organometallics XXXX, XXX, XXX−XXX

for 8 h (homogeneous solution), and then the solvent was removed in vacuo. The sample was dried under vacuum at 60 °C overnight, yielding 333 mg of a blue powdery solid. Yield 86%. Crystals suitable for X-ray diffraction analysis were grown by evaporation of a THF/hexanes solution at ambient temperature. Elemental analysis: Calculated: C, 55.52; H, 8.08. Found: C, 55.94; H, 8.22%.

Synthesis of (R,R)-MeBPE-CrCl$_3$(THF) (13-Cr). $CrCl_3(THF)_3$ (360 mg, 0.97 mmol) was dissolved in 5 mL of THF giving a purple solution. To this solution was added dropwise a solution of the (*R*,*R*)-MeBPE ligand (**13**) (250 mg, 0.97 mmol) in 5 mL of THF. The solution color immediately changed from purple to a dark cobalt blue. The solution was allowed to stir overnight at ambient temperature. The THF was removed in vacuo, and the residue was redissolved in a minimal amount of THF (∼5 mL) followed by addition of hexanes (∼30 mL). The resulting suspension was filtered through a frit, and then the solvent was removed from the filtrate in vacuo to yield 299.9 mg of a blue solid. Yield 63.4%. Elemental analysis: Calculated: C, 44.23; H, 7.42. Found: C, 44.08; H, 7.21%.

Synthesis of Complex 17-Cr. $CrCl_3(THF)_3$ (199.0 mg, 0.53 mmol) was dissolved in 5 mL of THF giving a purple solution. To this solution was added a solution of 150.0 mg of ligand (*S*,*S*)-**17** (0.53 mmol) dissolved in 5 mL of THF. The reaction mixture was allowed to stir overnight at elevated temperature (65 °C). The reaction mixture was filtered through a frit, and the solvent was removed from the filtrate in vacuo, yielding 33.3 mg of a blue solid. Yield 12.3%. Crystals suitable for a single-crystal X-ray diffraction study were obtained via slow evaporation of a chloroform solution of the complex at ambient temperature. Elemental analysis: Calculated: C, 47.12; H, 6.53. Found: C, 47.04; H, 6.72%.

Synthesis of (S,S)-MeDuPhos-Cr(CO)$_4$ (10-Cr(CO)$_4$). 1,2-Bis((2*S*,5*S*)-2,5-dimethylphospholano)benzene ((*S*,*S*)-MeDuPhos ligand, **10**) (0.4933 g, 1.61 mmol) and $Cr(CO)_6$ (0.7086 g, 3.22 mmol) were combined in toluene (8 mL). The reaction mixture was heated overnight (20 h) at 110 °C. A ^{31}P NMR spectrum showed ∼66% conversion to the desired product. During the course of the reaction, unreacted $Cr(CO)_6$ sublimed to the top of the vial, and the vial was shaken every few hours to return the $Cr(CO)_6$ back into the reaction solution. The solution was heated for another 24 h at 120 °C. The ^{31}P NMR spectrum showed complete conversion to the desired product. The solution was cooled to room temperature overnight (white $Cr(CO)_6$ crystals were at the top of the vial). Hexane (8 mL) was added, and the solution was filtered. Within minutes a light yellow highly crystalline material appeared. A small amount (0.5 mL) of the supernatant was filtered (syringe filter) into an 8 mL vial, which was set aside at ambient temperature. Within 2 h large crystals grew, which were analyzed by X-ray diffraction. The vial containing the remainder of the reaction mixture was placed into a freezer (−30 °C) overnight. The product (light yellow crystals) was collected on a frit, washed with hexane (2 × 3 mL), and dried under reduced pressure to give 0.520 g. Yield 68.7%. NMR spectra show formation of clean product. ^{1}H NMR (500 MHz, chloroform-*d*) δ 7.71 (dq, J = 6.0, 3.1 Hz, 2H), 7.51 (ddt, J = 7.7, 4.2, 2.1 Hz, 2H), 2.86 (tq, J = 12.3, 6.5, 6.0 Hz, 2H), 2.54 (dtd, J = 13.2, 7.6, 7.2, 3.9 Hz, 2H), 2.39−2.12 (m, 4H), 1.75−1.58 (m, 4H), 1.43 (dd, J = 17.6, 7.0 Hz, 6H), 0.72 (dd, J = 13.8, 7.0 Hz, 6H). ^{13}C NMR (126 MHz, chloroform-*d*) δ 229.33 (t, J = 8.1 Hz), 221.57 (t, J = 13.5 Hz), 144.48 (dd, J = 31.4, 28.9 Hz), 131.46 (t, J = 13.0 Hz), 129.41, 42.82 (dd, J = 13.9, 11.9 Hz), 42.25 (dd, J = 12.5, 9.9 Hz), 36.73 (t, J = 2.2 Hz), 36.62, 18.24 (t, J = 5.5 Hz), 14.82. ^{31}P NMR (162 MHz, benzene-d_6) δ 97.76. Elemental analysis for $C_{22}H_{28}CrNO_4P_2$: Calculated: C, 56.17; H, 6.00. Found: C, 55.87; H, 5.92%.

X-ray Structure Determination. X-ray intensity data were collected on a Bruker SMART diffractometer using Mo Kα radiation (λ = 0.710 73 Å) and an APEXII CCD area detector. Raw data frames were read by the program SAINT[31] and integrated using three-dimensional (3D) profiling algorithms. The resulting data were reduced to produce hkl reflections and their intensities and estimated standard deviations. The data were corrected for Lorentz and polarization effects, and numerical absorption corrections were applied based on indexed and measured faces. The structures were solved and refined in SHELXTL6.1, using full-matrix least-squares refinement. The non-H atoms were refined with anisotropic thermal parameters, and all of the H atoms were calculated in idealized positions and refined riding on their parent atoms. The refinements were performed using F^2 rather than F values. In each case R_1 was calculated to provide a reference to the conventional R value, but its function was not.

■ ASSOCIATED CONTENT

Supporting Information

The Supporting Information is available free of charge at https://pubs.acs.org/doi/10.1021/acs.organomet.9b00722.

Synthesis and characterization data, complete reactor data, and example activity and selectivity calculations (PDF)

Accession Codes

CCDC 1958676−1958686 and 1960323−1960324 contain the supplementary crystallographic data for this paper. These data can be obtained free of charge via www.ccdc.cam.ac.uk/data_request/cif, or by emailing data_request@ccdc.cam.ac.uk, or by contacting The Cambridge Crystallographic Data Centre, 12 Union Road, Cambridge CB2 1EZ, UK; fax: + 44 1223 336033.

■ AUTHOR INFORMATION

Corresponding Authors

Mari S. Rosen − *Corporate R&D, The Dow Chemical Company, Midland, Michigan 48667, United States;* orcid.org/0000-0002-1153-3051; Email: msrosen@dow.com

Jerzy Klosin − *Corporate R&D, The Dow Chemical Company, Midland, Michigan 48667, United States;* orcid.org/0000-0002-9045-7308; Email: jklosin@dow.com

Authors

Scott D. Boelter − *Corporate R&D, The Dow Chemical Company, Midland, Michigan 48667, United States*

Dan R. Davies − *Corporate R&D, The Dow Chemical Company, Midland, Michigan 48667, United States*

Peter Margl − *Corporate R&D, The Dow Chemical Company, Midland, Michigan 48667, United States*

Kara A. Milbrandt − *Corporate R&D, The Dow Chemical Company, Midland, Michigan 48667, United States*

Darrek Mort − *Corporate R&D, The Dow Chemical Company, Midland, Michigan 48667, United States*

Britt A. Vanchura, II − *Corporate R&D, The Dow Chemical Company, Midland, Michigan 48667, United States*

David R. Wilson − *Corporate R&D, The Dow Chemical Company, Midland, Michigan 48667, United States*

Molly Wiltzius − *Corporate R&D, The Dow Chemical Company, Midland, Michigan 48667, United States*

Complete contact information is available at: https://pubs.acs.org/10.1021/acs.organomet.9b00722

Notes

The authors declare no competing financial interest.

■ ACKNOWLEDGMENTS

We thank Dr. D. Laitar for assistance with the refinement of X-ray structures.

REFERENCES

(1) Greiner, E.; Bland, A.; Zhang, E.; Kumamoto, T. *Linear alpha-Olefins, Chemical Economic Handbook;* IHS Chemical, 2017.

(2) McGuinness, D. S. Olefin Oligomerization via Metallacycles: Dimerization, Trimerization, Tetramerization, and Beyond. *Chem. Rev.* **2011**, *111*, 2321−2341.

(3) Sydora, O. L. Selective Ethylene Oligomerization. *Organometallics* **2019**, *38*, 997−1010.

(4) (a) Bollmann, A.; Blann, K.; Dixon, J. T.; Hess, F. M.; Killian, E.; Maumela, H.; McGuinness, D. S.; Morgan, D. H.; Neveling, A.; Otto, S.; Overett, M.; Slawin, A. M. Z.; Wasserscheid, P.; Kuhlmann, S. Ethylene Tetramerization: A New Route to Produce 1-Octene in Exceptionally High Selectivities. *J. Am. Chem. Soc.* **2004**, *126*, 14712−14713. (b) Blann, K.; Bollmann, A.; Dixon, J. T.; Neveling, A.; Morgan, D. H.; Maumela, H.; Killian, E.; Hess, F. M.; Otto, S.; Pepler, L.; Mahomed, H. A.; Overett, M. J.; Green, M. J. International Patent Application WO 2004/056478, July 8, 2004 (Sasol Technology).

(5) Agapie, T. Selective Ethylene Oligomerization: Recent Advances in Chromium Catalysis and Mechanistic Investigations. *Coord. Chem. Rev.* **2011**, *255*, 861−880.

(6) Cloete, N.; Visser, H. G.; Engelbrecht, I.; Overett, M. J.; Gabrielli, W. F.; Roodt, A. Ethylene Tri- and Tetramerization: A Steric Parameter Selectivity Switch from X-ray Crystallography and Computational Analysis. *Inorg. Chem.* **2013**, *52*, 2268−2270.

(7) Boelter, S. D.; Davies, D. R.; Milbrandt, K. A.; Wilson, D. R.; Wiltzius, M.; Rosen, M. S.; Klosin, J. Evaluation of Bis(phosphine) Ligands for Ethylene Oligomerization: Discovery of Alkyl Phosphines as Effective Ligands for Ethylene Tri- and Tetramerization. *Organometallics* **2020**, DOI: 10.1021/acs.organomet.9b00721.

(8) Overett, M. J.; Blann, K.; Bollmann, A.; Dixon, J. T.; Hess, F.; Killian, E.; Maumela, H.; Morgan, D. H.; Neveling, A.; Otto, S. Ethylene Trimerisation and Tetramerisation Catalysts with Polar-Substituted Diphosphinoamine Ligands. *Chem. Commun.* **2005**, 622−624.

(9) Blann, K.; Bollmann, A.; de Bod, H.; Dixon, J. T.; Killian, E.; Nongodlwana, P.; Maumela, M. C.; Maumela, H.; McConnell, A. E.; Morgan, D. H.; Overett, M. J.; Pretorius, M.; Kuhlmann, S.; Wasserscheid, P. Ethylene Tetramerisation: Subtle Effects Exhibited by N-Substituted Diphosphinoamine Ligands. *J. Catal.* **2007**, *249*, 244−249.

(10) Overett, M. J.; Blann, K.; Bollmann, A.; de Villiers, R.; Dixon, J. T.; Killian, E.; Maumela, M. C.; Maumela, H.; McGuinness, D. S.; Morgan, D. H.; Rucklidge, A.; Slawin, A. M. Z. Carbon-Bridged Diphosphine Ligands for Chromium-Catalysed Ethylene Tetramerisation and Trimerisation Reactions. *J. Mol. Catal. A: Chem.* **2008**, *283*, 114−119.

(11) Sydora, O. L.; Jones, T. C.; Small, B. L.; Nett, A. J.; Fischer, A. A.; Carney, M. J. Selective Ethylene Tri-/Tetramerization Catalysts. *ACS Catal.* **2012**, *2*, 2452−2455.

(12) Zhang, J.; Wang, X.; Zhang, X.; Wu, W.; Zhang, G.; Xu, S.; Shi, M. Switchable Ethylene Tri-/Tetramerization with High Activity: Subtle Effect Presented by Backbone-Substituent of Carbon-Bridged Diphosphine Ligands. *ACS Catal.* **2013**, *3*, 2311−2317.

(13) Alam, F.; Zhang, L.; Wei, W.; Wang, J.; Chen, Y.; Dong, C.; Jiang, T. Catalytic Systems Based on Chromium(III) Silylated-Diphosphinoamines for Selective Ethylene Tri-/Tetramerization. *ACS Catal.* **2018**, *8*, 10836−10845.

(14) (a) Han Taek Kyu, K. R.; Ok Myung Ahn, K. R.; Chae Sung Seok, K. R.; Kang Sang Ook, K. R.; Jung Jae Ho, K. R. International Patent Application WO2008088178A1, July 24, 2008 (SK Energy). (b) Gao, X.; Carter, C. A. G.; Lee, D. International Patent Application WO2010/034102, April 1, 2010 (Nova Chemicals). (c) Cho, M. S.; Lee, Y. H.; Sa, S. P.; Kwon, H. Y.; Cho, K. J.; Kim, S. Y.; Lee, S. M.; Lee, K. S.; Lim, K. S. U.S. Patent Application 2015/0298110, Oct 22, 2015 (LG Chem).

(15) A small set of alkyl bis-phosphines has been previously evaluated by Overett et al. (ref 10) and in the following: (a) McGuinness, D. S.; Overett, M.; Tooze, R. P.; Blann, K.; Dixon, J. T.; Slawin, A. M. Z. Ethylene Tri- and Tetramerization with Borate Cocatalysts: Effects on Activity, Selectivity, and Catalyst Degradation Pathways. *Organometallics* **2007**, *26*, 1108−1111. (b) Weng, Z.; Teo, S.; Andy Hor, T. S. Chromium(III)-Catalysed Ethylene Tetramerization Promoted by Bis(Phosphino) Amines with an N-Functionalized Pendant. *Dalton Trans.* **2007**, 3493−3498.

(16) PNP ligands containing unsaturated phosphacycles have been previously reported: Stennett, T. E.; Hey, T. W.; Ball, L. T.; Flynn, S. R.; Radcliffe, J. E.; McMullin, C. L.; Wingad, R. L.; Wass, D. F. N,N-Diphospholylamines—A New Family of Ligands for Highly Active, Chromium-Based, Selective Ethene Oligomerisation Catalysts. *ChemCatChem* **2013**, *5*, 2946−2954.

(17) Samples were prepared at a concentration of ∼20 mg/mL, and 256 scans were used to acquire the spectra.

(18) When MeDuPhos-$CrCl_3$(THF) is recrystallized from CH_2Cl_2, its corresponding dimer $[(S,S)$-MeDuPhos-$CrCl_2(\mu\text{-Cl})]_2$ is formed, which was characterized by elemental analysis and X-ray crystallography. See Supporting Information for details.

(19) There are two independent molecules in the asymmetric unit for 11-Cr. The maximum deviations from the least-squares plane for the second molecule is 0.13 Å for C2. For **12-Cr**, there are four independent molecules in the asymmetric unit. The maximum deviations from the least-squares plane for the other three molecules are 0.14, 0.04, and 0.04 Å for the P2 atom. There is very little deviation from planarity for two of the four molecules of **12-Cr.**

(20) See Supporting Information for details.

(21) Bowen, L. E.; Haddow, M. F.; Orpen, A. G.; Wass, D. F. One Electron Oxidation of Chromium N,N-Bis(Diarylphosphino)Amine and Bis(Diarylphosphino)Methane Complexes Relevant to Ethene Trimerisation And Tetramerisation. *Dalton Trans.* **2007**, 1160−1168.

(22) MMAO-3A is the most commonly used and effective activator for chromium-based ethylene oligomerization catalysts. Activators commonly used in olefin polymerization, such as ammonium borates, have also been investigated in ethylene tetramerization reactions: (a) Kim, T. H.; Lee, H. M.; Park, H. S.; Kim, S. D.; Kwon, S. J.; Tahara, A.; Nagashima, H.; Lee, B. Y. MAO-Free and Extremely Active Catalytic System for Ethylene Tetramerization. *Appl. Organomet. Chem.* **2019**, *33*, No. e4829. (b) Park, H. S.; Kim, T. H.; Baek, J. W.; Lee, H. J.; Kim, T. J.; Ryu, J. Y.; Lee, J.; Lee, B. Y. Extremely Active Ethylene Tetramerization Catalyst Avoiding the Use of Methylaluminoxane: $[iPrN\{P(C_6H_4\text{-}p\text{-}SiR_3)_2\}_2CrCl_2]^+[B(C_6F_5)_4]^-$. *ChemCatChem.* **2019**, *11*, 1−10. Other reports investigating the role of the cocatalyst for this chemistry include McGuinness et al. (ref 15a) and the following: (c) Ewart, S. W.; Dixon, J. T.; de Bod, H.; Evans, S. J.; Kolthammer, B. W. S.; Morgan, D. H.; Hanton, M. J.; Smith, D. M.; Gabrielli, W. F. WO/2010/092554A1, 2010 (Sasol Technology). (d) McGuinness, D. S.; Rucklidge, A. J.; Tooze, R. P.; Slawin, A. M. Z. Cocatalyst Influence in Selective Oligomerization: Effect on Activity, Catalyst Stability, and 1-Hexene/1-Octene Selectivity in the Ethylene Trimerization and Tetramerization Reaction. *Organometallics* **2007**, *26*, 2561−2569. (e) Schofer, S. J.; Day, M. W.; Henling, L. M.; Labinger, J. A.; Bercaw, J. E. Ethylene Trimerization Catalysts Based on Chromium Complexes with a Nitrogen-Bridged Diphosphine Ligand Having ortho-Methoxyaryl or ortho-Thiomethoxy Substituents: Well-Defined Catalyst Precursors and Investigations of the Mechanism. *Organometallics* **2006**, *25*, 2743−2749. (f) Hirscher, N. A.; Agapie, T. Stoichiometrically Activated Catalysts for Ethylene Tetramerization using Diphosphinoamine Ligated Cr Tris(hydrocarbyl) Complexes. *Organometallics* **2017**, *36*, 4107−4110. (g) Hirscher, N. A.; Perez Sierra, D.; Agapie, T. Robust Chromium Precursors for Catalysis: Isolation and Structure of a Single-Component Ethylene Tetramerization Precatalyst. *J. Am. Chem. Soc.* **2019**, *141*, 6022−6029.

(23) Clavier, H.; Nolan, S. P. Percent Buried Volume for Phosphine and N-Heterocyclic Carbene Ligands: Steric Properties in Organometallic Chemistry. *Chem. Commun.* **2010**, *46*, 841−861.

(24) Poater, A.; Cosenza, B.; Correa, A.; Giudice, S.; Ragone, F.; Scarano, V.; Cavallo, L. SambVca: A Web Application for the Calculation of the Buried Volume of N-Heterocyclic Carbene Ligands. *Eur. J. Inorg. Chem.* **2009**, 1759−1766.

https://dx.doi.org/10.1021/acs.organomet.9b00722
Organometallics XXXX, XXX, XXX−XXX

(25) Two model systems were chosen for $\%V_{bur}$ calculations. The first model system used the crystal structures of ligand-$CrCl_3$(THF) complexes. $\%V_{bur}$ calculations were performed using the SambVca program (https://www.molnac.unisa.it/OMtools/sambvca2.1/index.html) as described in *Organometallics* 2016, *35*, 2286−2293 and *Nat. Chem.* 2019, *11*, 872−879. As recommended in this literature, atomic radii were scaled by 1.17, and a sphere of radius of 3.5 Å was used. Spheres of larger radii (up to 5 Å) were also evaluated given the distance of the phospholane substituents to the Cr center. The second model system used ligand-chromacyclononane complexes. The metallacyclononane intermediate was chosen as a model system, because it is one of the crucial intermediates leading to the formation of octene. In this instance, %Vbur was calculated based on DFT-optimized metallacyclononane intermediates as described in the Supporting Information. Correlations between experimental values (such as 1-octene and 1-hexene selectivities) and %Vbur values obtained from analysis of the ligand-$CrCl_3$(THF) crystal structures and from the ligand-chromacyclononane species were sought. While the best correlations were obtained from the use of the (1-octene + cyclics)/1-hexene ratio (Supporting Information Figure 43), these correlations were weak, and strong correlations between the %Vbur steric descriptor and experimental values were not observed, despite the experimental observed trends.

(26) (a) Britovsek, G. J. P.; McGuinness, D. S.; Wierenga, T. S.; Young, C. T. Single- and Double-Coordination Mechanism in Ethylene Tri- and Tetramerization with Cr/PNP Catalysts. *ACS Catal.* **2015**, *5*, 4152−4166. (b) Britovsek, G. J. P.; McGuinness, D. S. A DFT Mechanistic Study on Ethylene Tri- and Tetramerization with Cr/PNP Catalysts: Single versus Double Insertion Pathways. *Chem. - Eur. J.* **2016**, *22*, 16891−16896.

(27) Hirscher, N. A.; Labinger, J. A.; Agapie, T. Isotopic Labelling in Ethylene Oligomerization: Addressing the Issue of 1-Octene vs. 1-Hexene Selectivity. *Dalton Trans.* **2019**, *48*, 40−44.

(28) Elowe, P. R.; McCann, C.; Pringle, P. G.; Spitzmesser, S. K.; Bercaw, J. E. Nitrogen-Linked Diphosphine Ligands with Ethers Attached to Nitrogen for Chromium-Catalyzed Ethylene Tri- and Tetramerizations. *Organometallics* **2006**, *25*, 5255−5260.

(29) Gunasekara, T.; Kim, J.; Preston, A.; Steelman, D. K.; Medvedev, G. A.; Delgass, W. N.; Sydora, O. L.; Caruthers, J. M.; Abu-Omar, M. M. Mechanistic Insights into Chromium-Catalyzed Ethylene Trimerization. *ACS Catal.* **2018**, *8*, 6810−6819.

(30) Overett, M. J.; Blann, K.; Bollmann, A.; Dixon, J. T.; Haasbroek, D.; Killian, E.; Maumela, H.; McGuinness, D. S.; Morgan, D. H. Mechanistic Investigations of the Ethylene Tetramerisation Reaction. *J. Am. Chem. Soc.* **2005**, *127*, 10723−10730.

(31) Sheldrick, G. M. *SHELXTL6.1,* Crystallographic software package; Bruker AXS, Inc.: Madison, WI, 2008.

https://dx.doi.org/10.1021/acs.organomet.9b00722
Organometallics XXXX, XXX, XXX−XXX